IMPLADENT LTD.
ADVANCING THE SCIENCE OF IMPLANTOLOGY™

Student Research Award in the Hospital Intern, Resident or Clinical Fellow Category, 16th Annual Meeting of the Society for Biomaterials, Charleston, SC, May 20–23, 1990

A new canine model to evaluate the biological response of intramedullary bone to implant materials and surfaces

Jeffrey M. Spivak, John L. Ricci, Norman C. Blumenthal, and Harold Alexander
Department of Bioengineering, Hospital for Joint Diseases Orthopaedic Institute, New York, New York 10003

A new canine model utilizing an implantable chamber with multiple bone ingrowth channels has been used to study the response of intramedullary bone to various implant materials and surfaces.

The first group of dogs received implants containing channels lined by smooth-surfaced coupons of titanium, titanium alloy, sputter-hydroxyapatite-coated (HA-coated) titanium alloy, and polyethylene. A pattern of early initial bone ingrowth by 2 weeks, becoming maximal at 6 to 12 weeks with remodeling to a more mature lamellar bone, and later resorption by 24 weeks was seen for all test groups, with fibrous tissue interfaces covering the smooth test coupons at all time points. Significantly increased bone ingrowth in the sputter-HA coated group was found only at 6 weeks.

The second group of dogs received implants with channels lined by surface-roughened coupons of either titanium or plasma-HA-coated titanium, half of which were also packed with a crystalline-HA grouting at the time of surgery. At both 6 and 12 weeks, bone ingrowth was greatly enhanced by the presence of the plasma-HA coating or the crystalline-HA grouting as compared to the uncoated titanium channels. Histologically, bone was seen to bond directly to the plasma-HA coating and the crystalline-HA grouting. A thin fibrous tissue layer was noted between bone and the titanium in most areas, but evidence of direct bone contact to the metal surface was seen. Mechanical testing in tension of intact coupon–bone–coupon units revealed significant strength of the bone–plasma–HA bond, with failure initiating at the metal–HA interface with forces of 15.3 N at 6 weeks, increasing to 44.8 N at 12 weeks. Plasma-HA-lined channels with crystalline-HA packing required similar forces for failure. No significant adhesion strength was noted for the titanium channels at 6 weeks, and only the crystalline-HA-filled channels displayed measurable strength of the bone–titanium interface at 12 weeks, with a force of 9 N needed for failure.

Winner of AOA-Zimmer 1990 Resident Travel Award.

Journal of Biomedical Materials Research, Vol. 24, 1121–1149 (1990)
© 1990 John Wiley & Sons, Inc. CCC 0021-9304/90/091121-29$04.00

INTRODUCTION

Complications of acrylic cement fixation have led to the search for newer, more biologically compatible methods of long-term fixation of orthopedic implants. Various materials and surface coatings believed to be biocompatible or bioactive with surrounding intramedullary bone are being used in new implant designs that rely on either porous ingrowth or direct biologic bonding of bone to the implant surface.[1,2] New metals, ceramics, and composite materials are being tested for use in orthopedic implants.[3–6]

Recent interest has arisen in the orthopedic community in the use of hydroxyapatite (HA) coatings on orthopedic implants to promote bone ingrowth and direct biologic fixation.[2,4,7–9] The term *hydroxyapatite* refers to a diverse group of ceramic calcium phosphate compounds, all similar to the natural hydroxyapatite of bone [$Ca_{10}(PO_4)_6(OH)_2$], but differing in their exact chemical composition and crystalline structure depending on the conditions under which they are formed.[10] Studies have indicated direct bone bonding to HA compounds[11–13] and have shown enhanced porous ingrowth and increased failure strengths using high-temperature plasma-sprayed HA coatings.[14] Microporous particulate HA grouting has also shown to enhance early stabilization of intramedullary threaded implants.[15]

Implantable chambers have been used previously in the study of bone tissue.[16–21] Commercially pure (CP) titanium is most often used to form the chamber, because of its proven biocompatibility and its apparent "osteointegration" with surrounding bone.[22–28] However, the effects (if any) of titanium on the processes of bone growth and repair being studied are not fully known. The poisoning of HA formation by various ionic metal species, including titanium, has been demonstrated through *in vitro* testing.[29]

The purpose of this study was to develop an animal model for studying the intramedullary bone response to current and prospective implant materials and surfaces using an implantable chamber housing multiple bone ingrowth channels. Ultrahigh-molecular-weight (UHMW) polyethylene was chosen as the outer chamber material, manufactured to incorporate thin coupons of various test materials to be the walls lining multiple tissue ingrowth channels, where the test coupons could be varied from channel to channel as desired prior to implantation. Test materials chosen for the initial implant trials included four smooth-surfaced materials—including coupons of CP titanium, titanium (Ti-6Al-4V) alloy, sputter-HA-coated titanium alloy, and UHMW polyethylene—and two surface-roughened materials, represented by coupons of CP titanium and plasma-HA-coated CP titanium. The effect of crystalline-HA in the ingrowth channels was also examined.

MATERIALS AND METHODS

Sixteen skeletally mature mongrel dogs were used in this study. Preoperative x-rays showed closed growth plates and no skeletal abnormalities of the distal femurs in all cases.

ingrowth channels were oriented perpendicular to the long axis of the femur; the channel openings faced the endosteal surface of the intact anterior and posterior cortices (Fig. 2).

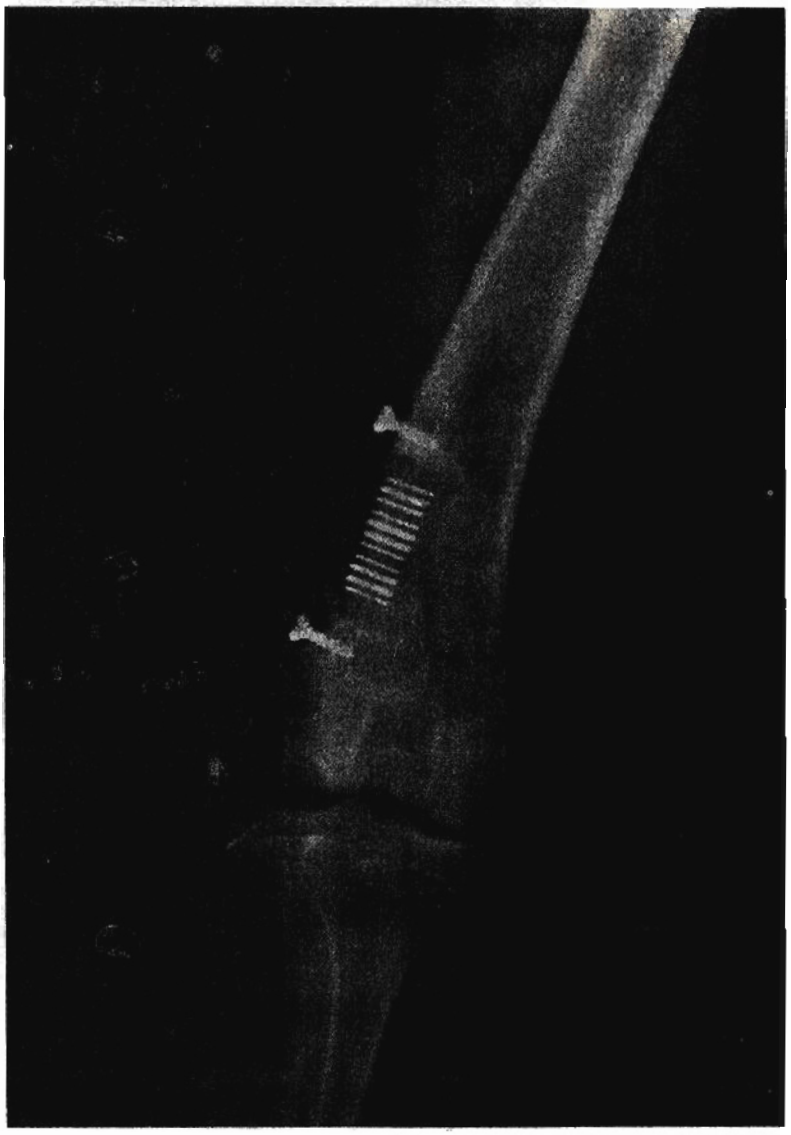

(a)

Figure 2. Six weeks post chamber implantation in the lateral distal femur. (a) AP and (b) lateral x-rays showing the intramedullary position of the ingrowth channels *in situ*, with the channel openings adjacent to the intact anterior and posterior cortices. Note the mild bone remodeling seen around the implant.

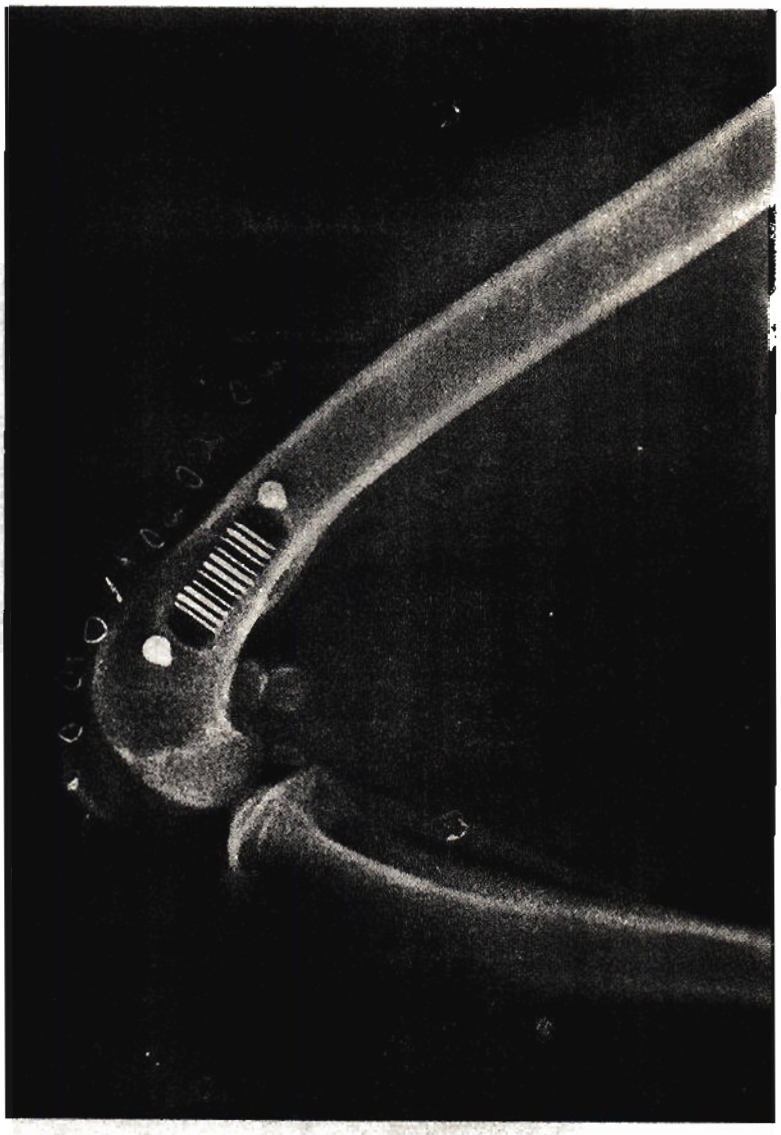

(b)

Figure 2. (continued)

All operations were performed by a single surgeon, and the operative technique used was identical for each dog. The supracondylar region of the femur was approached by a direct lateral skin incision extending distally along the lateral border of the patella tendon to the tibial tubercle. After incision of the fascia lata and lateral patellar retinaculum, the lateral cortex of the distal femur was reached through the avascular and internervous plane

between the vastus lateralis and the lateral hamstrings. The patella was dislocated medially to facilitate the exposure. The lateral periosteum was incised longitudinally, and both anterior and posterior flaps were carefully elevated. A drill template was fixed to the lateral metaphysis using Kirshner wires, and a rectangle measuring 8 × 25 mm was marked by serial drill-holes made with a titanium-coated drill bit. The template was always positioned to allow the most distal placement of the implants in the femoral metaphysis, equidistant between the anterior and posterior cortices. The drill holes were connected with an osteotome, and the lateral cortical window was removed. An osteotome was then used to remove a 10-mm-deep rectangle of cancellous metaphyseal bone flush with the sides of the defect. The sides were carefully enlarged as needed to allow for the snug insertion of a metal trial implant. The blood filling the intramedullary defect was used to fill the channels in the implant, so that no air was left in the channels, and the implant was carefully inserted. Unicortical 2.7-mm titanium bone screws (Synthes) were used to fix the implant both proximally and distally, preventing any implant motion. Closure was done using interrupted resorbable sutures to repair the fascia lata and patellar retinaculum and to reapproximate the subcutaneous tissue, and interrupted 3-0 stainless-steel sutures were used for the skin. Bilateral procedures were done on all animals, which were allowed full postoperative weight-bearing. All were given intramuscular antibiotics (penicillin-G procaine) preoperatively and for the first 5 postoperative days.

The first study group included 12 dogs, whose implants contained channels lined by smooth-finished coupons of four test materials: CP titanium, titanium alloy, titanium alloy with a 4- to 6-μm-thick layer of low-temperature, vapor-deposited hydroxyapatite ("sputter-HA-coated titanium alloy"), and medical-grade UHMW polyethylene. Scanning electromicroscopic (SEM) examination of the coupon surfaces of all four test coupons prior to implantation showed them to have similar surface finishes. Coupon placement was randomized to minimize anatomical effects of ingrowth channel position, but both surfaces of any given channel were always lined by coupons of the same test material.

One dog was killed 2 weeks postoperatively, four dogs each were killed 6 and 12 weeks postoperatively, and three dogs were killed 24 weeks postoperatively. The femurs were harvested intact and kept on ice. A diamond wire saw was then used to isolate each implant from surrounding bone. Faxitron x-ray images of the intact implants were obtained with the x-ray film perpendicular to the tissue–coupon interface (see Figs. 6A and 11). Most of the implants were then carefully disassembled, and the contents of the individual channels, consisting of fibrous tissue and newly developed bone which had grown in from the adjacent medullary space, were removed. These specimens were then re-x-rayed with the film parallel to the tissue–coupon interface. Representative specimens were then fixed in 10% formalin for undecalcified light microscopy and microradiographic examination, and the remainder were fresh-frozen for subsequent ash weight analy-

sis. These specimens were weighed after 4 h at 110°C (dry weight) and again following 24 h at 600°C (ash weight), and the ash weight was expressed as the percent of total dry weight. The Faxitron images of the ingrowth tissue taken with the x-ray film parallel to the tissue–implant surface were enlarged and digitized using a Zeiss Videoplan digitizing system, and the amount of radiographically visible bone ingrowth through the 1-mm channel thickness was calculated and expressed as a percentage of the total available surface area. The 2-week implants and a portion of a 24-week implant were kept assembled and fixed in 10% formalin for light microscopy and microradiography with surrounding bone intact.

The second study group included four dogs whose implants contained channels lined by surface-roughened CP titanium, in which every other channel was coated with a 50- to 75-μm layer of plasma-sprayed hydroxyapatite (Impladent Inc., NY). Scanning EM analysis of both coated and uncoated titanium coupons revealed a similar surface roughness and general architecture. In each dog, one chamber was implanted "as is," with the intramedullary blood used to fill the channels prior to their insertion as previously described. For the other chamber, all 10 channels were hand-packed intraoperatively with a slurry made by mixing 5 cm^3 of intramedullary blood with 3 g of a sterile crystalline hydroxyapatite (OsteoGen®, Impladent Inc., NY), just prior to implantation into the femur.

Two dogs each were killed 6 and 12 weeks postoperatively. The femurs were harvested, kept on ice, and the implants were isolated from surrounding bone as previously described. Faxitron x-rays were obtained with surrounding bone intact to qualitatively assess the degree of bone ingrowth into the channels. After isolation of the intact implant using a diamond wire saw, the chambers were carefully dismantled. A special effort was made to preserve the two tissue–test coupon interfaces intact for each ingrowth channel. All specimens were maintained on ice and kept with normal saline as needed. When the entire coupon–tissue–coupon "sandwich" maintained its integrity at all interfaces, it was carefully placed into a specially designed holding jig (see Fig. 1) and mechanically tested to failure in tension using a Model 1321 Instron biaxial servohydraulic testing system at a rate of 2.5% total displacement per second. The failure surfaces of representative specimens following mechanical testing were examined by SEM. Following fixation in phosphate-buffered glutaraldehyde, the specimens were critical point dried, sputter coated with a 200-Å-thick layer of gold and examined using a JEOL JSM T-300 scanning electron microscope.

Representative specimens which were not mechanically tested were fixed in 10% formalin and embedded in methyl methacrylate. Undecalcified sections of these specimens were examined by microradiography and by light microscopy following staining with hematoxylin and eosin, or by the Masson trichrome or von Kossa techniques. Other specimens were fixed in cacodylate-buffered glutaraldehyde and processed for transmission electromicroscopy (TEM). TEM of the growing bone front was done using a JEOL 100 CX electron microscope.

Statistical analysis of the ash weight data, the apparent bone ingrowth area data, and the mechanical testing data was performed using a series of standard unpaired Student's *t*-tests to locate differences between sample groups.

RESULTS

Group I

All dogs healed uneventfully, were standing by the third postoperative day, and were walking comfortably with a normal gait by the fifth postoperative day. No infections or other complications occurred prior to sacrifice.

At 2 weeks, the blood which originally filled the ingrowth channels was completely replaced by a loose fibrous connective tissue. This contained a variable amount of newly formed bone which extended into the channels about 1 mm from each end, forming a network of thin trabeculae of woven bone. The majority of the trabecular surfaces were covered by a layer of osteoid tissue and by numerous osteoblasts (Fig. 3A). A 25- to 100-μm layer of fibrous tissue separated the bony structures from the surfaces of the sample coupons in all four sample groups.

By 6 weeks, the central connective tissue had become less cellular and more organized along the long axis of the ingrowth channel. The bony trabeculae were thickened, with more mature lamellar bone found near the openings of the channels, suggesting early remodeling (Fig. 3B). Well-defined marrow spaces were present within the ingrown bone tissue. A fibrous tissue layer of similar thickness was still evident covering the test coupons of all four test groups.

At 12 weeks, the central connective tissue appeared as mature, well-oriented fibrous tissue, intimately associated with and oriented to the ingrown bone. Osteoid was seen on less of the trabecular surfaces than in earlier time periods, and larger areas of mature lamellar bone with fewer marrow spaces were found. A 50- to 100-μm-thick layer of fibrous tissue was present at the coupon surfaces in all samples, with the exception of a single trabecular projection extending directly adjacent to the test coupon surface on only one sample examined, from the sputter-HA coated group.

By 24 weeks, the bone appeared thickened and mature, with minimal osteoid seen in the von Kossa-stained sections. The bone was of a dense lamellar structure, and evidence of osteoclastic resorption could be seen at the most central extent of the ingrown bone (Fig. 3C). The fibrous tissue layer along the test coupon surfaces was unchanged from previous time periods.

This same temporal pattern of bone ingrowth and remodeling was found in all four sample groups. In all chambers, no significant differences were noted relative to the anatomic channel position, from the most proximal to the most distal ends. Histologically, it was impossible to differentiate among the four sample groups, with one exception. The only difference

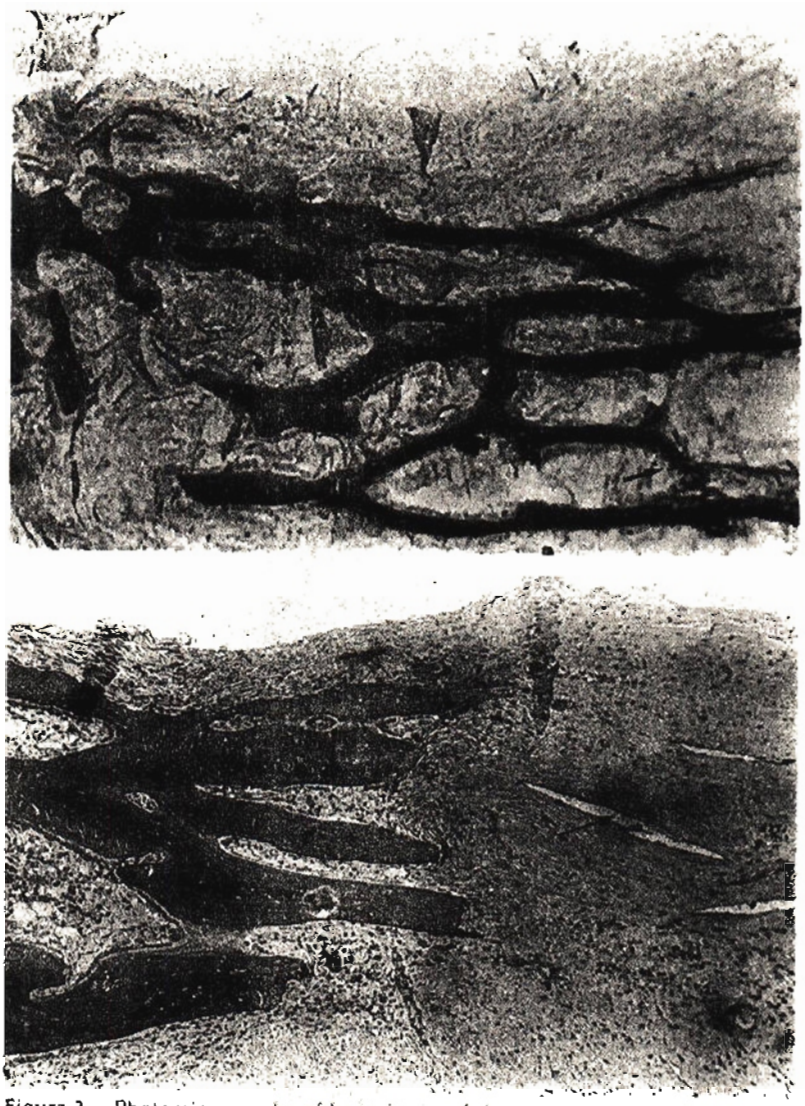

Figure 3. Photomicrographs of bone ingrowth into smooth-surfaced channels (a) At 2 weeks, a thin trabecular bone network (stained dark) and surrounding rim of lighter-staining osteoid (arrows) is seen. A 50-μm fibrous tissue layer is found between the upper extent of the bone and the space previously occupied by the test coupon (Masson; original magnification ×83). (b) By 6 weeks, the bone trabeculae are thicker, but a large amount of the surface is still covered by osteoid tissue and active osteoblasts. Note the fibrous tissue encapsulation of the sputter-HA coating, here seen having migrated into the center of the ingrowth channel after detaching from the coupon surface (arrow) (H & E, original magnification ×83). (c) At 24 weeks, osteoclastic resorption is seen at the central tip of bone ingrowth (H & E, original magnification ×529).

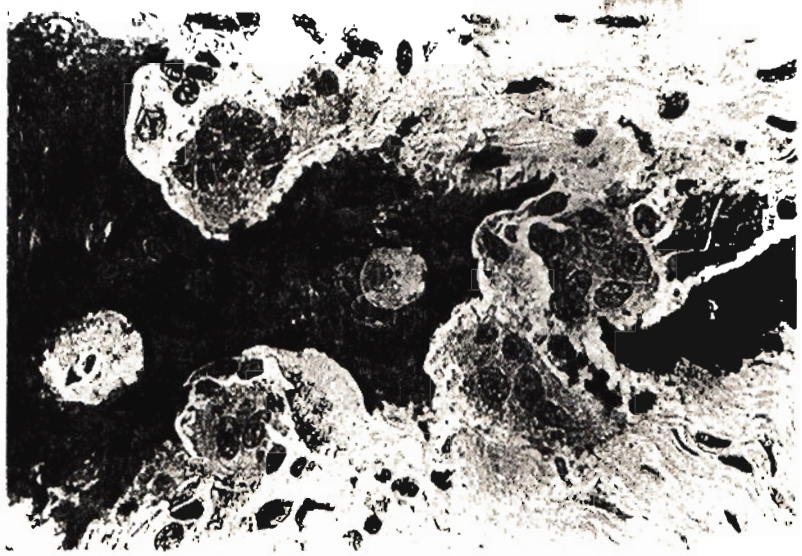

(c)

Figure 3. (continued)

seen under the light microscope was in the HA-sputter-coated group, where the coating was visibly flaked off into the fibrous tissue as early as 2 weeks postoperatively, and was still present in significant amounts at 24 weeks. The coating was surrounded by the central fibrous tissue in each specimen and was not in direct contact with the ingrown bone.

Ash weight analysis of the ingrowth tissue showed a high of 38% (on average for the four test groups) ash by weight at 6 weeks, decreasing to 19% at 24 weeks (Fig. 4). For all sample groups, a significant decrease in the percent ash weight was found when comparing the 6- and 24-week specimen groups (p values all $\leq .001$). The ash weight analysis showed a definite trend among the sample groups, with the tissue in the HA-coated channels having a higher ash weight for all dogs and at all time points. However, no statistically significant difference among the sample groups at any single time point was found. The trend of higher ash weights in the HA samples may be explainable at least in part by the HA coating itself, found to varying degrees within the samples.

Analysis of radiographically visible bone ingrowth paralleled the trends seen in the ash weight data, with an average of 42% of the channel area occupied by bone at 6 weeks, decreasing to only 21% by 24 weeks (Fig. 5). As with the ash weight data, each individual group showed a significant decline in visible ingrowth at 24 weeks as compared to 6 weeks (p values $\leq .003$). In comparing the different test groups within a single time period, a significant difference ($p \leq .03$) was seen only for the HA-coated channels (53% bone ingrowth) as compared to the others (36–40%) at 6 weeks.

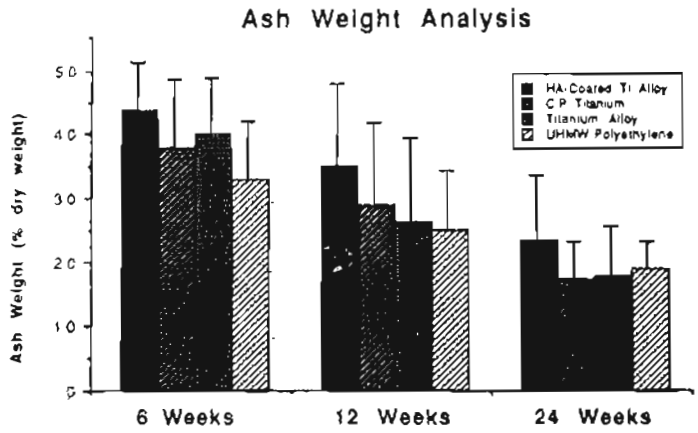

Figure 4. Ash weight analysis of bone ingrowth expressed as percentage of specimen dry weight at 6, 12, and 24 weeks (n = 9 samples per group per time). No significant differences were seen among sample groups at any given time period. Significant decreases were seen for 6-week vs. 24-week ash weights in all sample groups (p values ≤ .001).

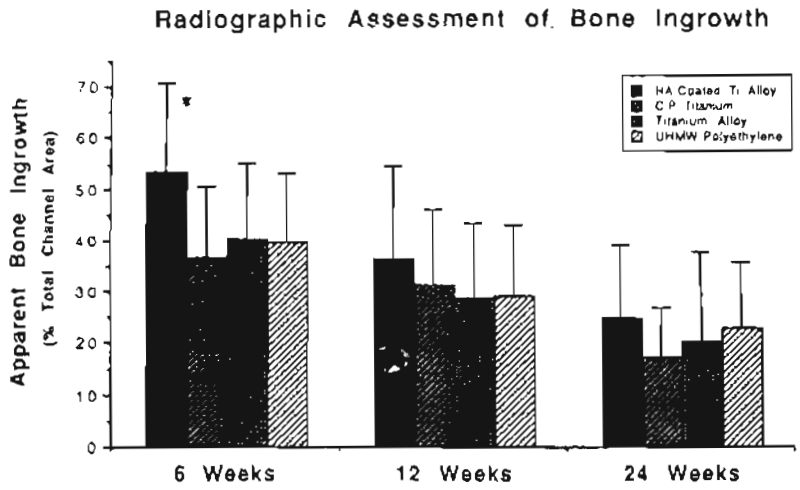

Figure 5. Radiographic assessment of bone ingrowth by area as seen on cross-sectional high-resolution Faxitron x-rays, expressed as percentage of available ingrowth area. Ingrown bone occupied significantly more channel area in the sputter-HA-lined channels at 6 weeks than in all others (*p ≤ .003). Decreases in area ingrowth paralleled ash weight decreases at 24 weeks as compared to 6 weeks for all sample types (p values ≤ 0.03).

In no specimen did bone fully fill the entire 5 × 8-mm area of the ingrowth channels. In fact, only a single sample (6 weeks) showed any continuous bridge of bone from one end of the channel to the other. In general,

the deepest penetration into the ingrowth channels was found at 6 weeks (2–4 mm from each side), declining to 1 mm or less by 24 weeks.

Group II

No operative complications occurred in this group. One 6-week dog sustained a midfemur fracture 4 days postoperatively, and underwent operative reduction and plate fixation on day 9. This complication occurred on the side containing the crystalline-HA grouting, and this limb was not included in the study.

At 6 weeks postimplantation, the plasma-HA-coated channels always contained larger amounts of radiographically visible ingrown bone than those channels lined with uncoated CP titanium, regardless of the channel's anatomic position within the implant chamber (Fig. 6). The presence of the crystalline HA grouting within the channel appeared to significantly enhance the ingrowth of bone in the CP titanium-lined channels (Fig. 7). In the plasma-HA-coated channels, the presence of the crystalline-HA grouting did not significantly enhance or block the increased bone ingrowth seen at 6 weeks. Histologically, a 200-μm layer of fibrous tissue was seen at the coupon surface in the 6-week CP titanium specimens, while those with the crystalline-HA grouting showed more bone ingrowth and a thinner layer of interposed connective tissue (Fig. 8). The ingrown bone was seen to be a vascular woven bone with thin trabeculae, surrounded on most of their surfaces by osteoid tissue and numerous osteoblasts. TEM of the central bone edge confirmed the formation of normal woven bone, with surrounding active osteoblasts and processes of osteoclasts indicating normal bone formation and remodeling. The plasma-HA-coated channels showed direct bone attachment to the HA coating on the light microscopic level (Fig. 9). Histologic examination of the crystalline-HA-filled channels showed bone ingrowth directly surrounding the crystals of HA without any visible interposing tissue and little evidence of resorption of the HA crystals (Fig. 10).

At 12 weeks, radiographic examination of the chambers revealed a complete bridge of bone within the HA-coated channels in all cases, regardless of the anatomic position of the channel (Fig. 11). The CP titanium channels showed greater bone ingrowth than the 6-week dogs, but displayed complete bridging by new bone in less than half of the channels. The presence of the crystalline-HA grouting within the channels significantly enhanced bone ingrowth in the CP titanium channels, promoting complete filling of all channels with new bone (Fig. 12). Light histologic examination confirmed the 6-week observation of ingrown bone directly attaching to the HA coating. In the CP titanium chambers, the thick fibrous tissue separating the ingrown bone from the coupon surface at 6 weeks was not found, and in many areas no intervening tissue was visible at the edges of the samples examined. In most areas, however, the ingrown bone was separated by the edge of the section by a thin layer of loose connective tissue, at most only a

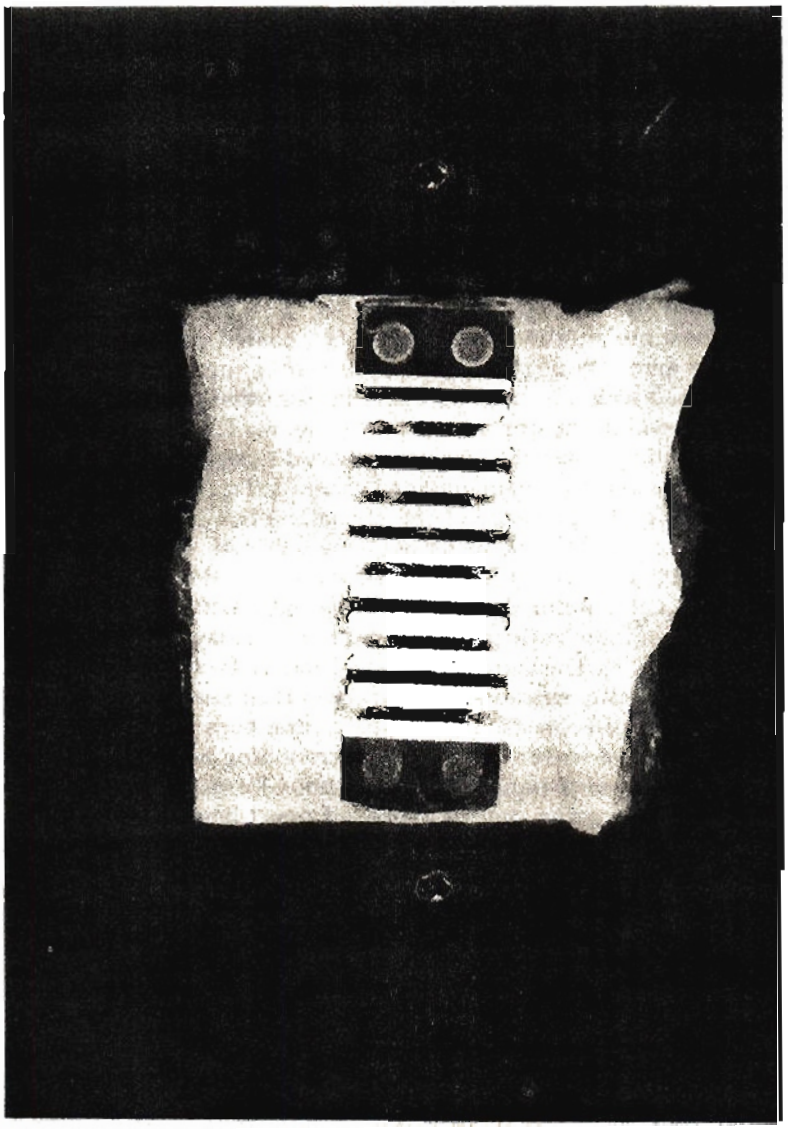

(a)

Figure 6. Radiographic comparisons of bone ingrowth into rough-surfaced CP titanium and plasma-HA coated CP-titanium-lined ingrowth channels at 6 weeks. (a) Faxitron high-resolution x-ray of an intact chamber with surrounding bone, showing increased bone ingrowth into the plasma-HA-lined channels (2nd, 4th, 6th, 8th, and bottom channels). (b) Comparison microradiographs demonstrating increased bone ingrowth in the plasma-HA-lined channel (bottom) vs. CP titanium (above) (original magnification ×33).

12

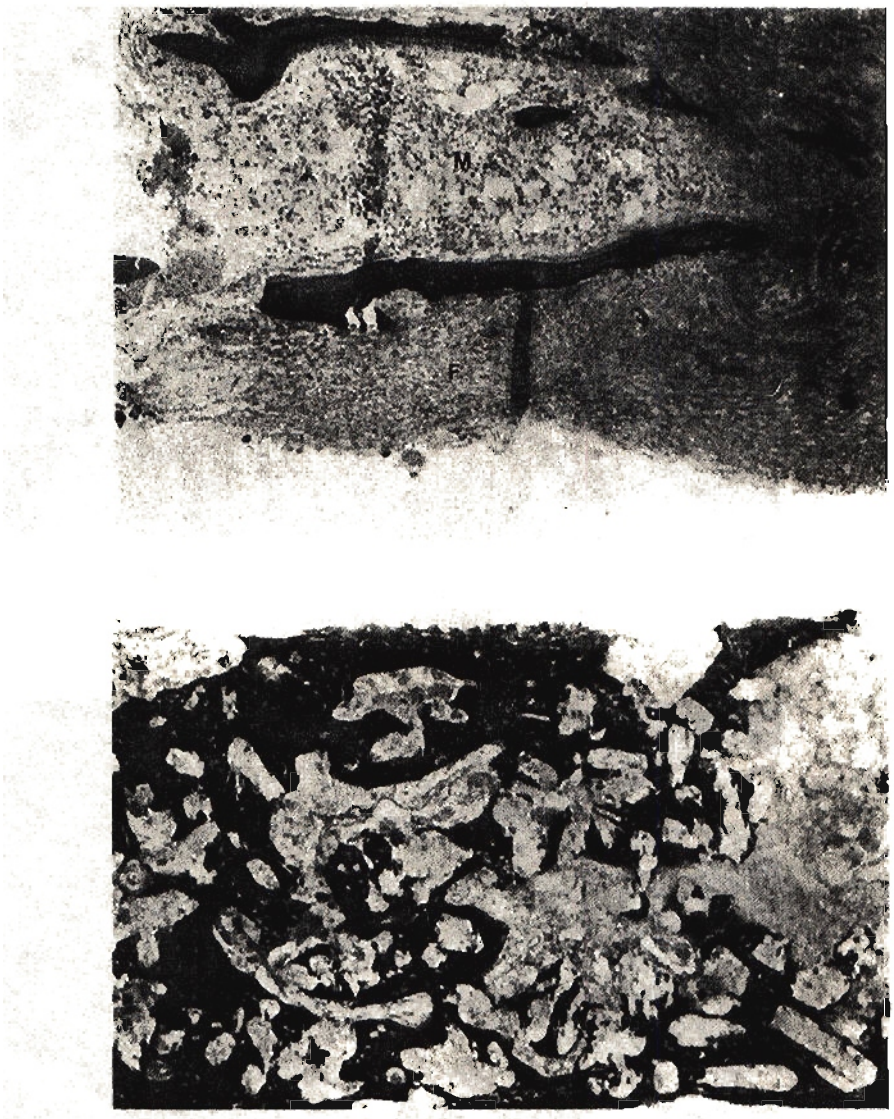

(b)

Figure 8. Photomicrographs of bone ingrowth at 6 weeks in the CP-titanium-lined channels. (a) An unfilled channel, adjacent to the intramedullary space on the left shows slender bone trabeculae surrounding a wide marrow space (M) and a 150-μm layer of fibrous tissue adjacent to the channel surface (F) (Masson, original magnification ×83). (b) Crystalline-HA-filled channel, showing enhanced bone ingrowth. There is little or no fibrous tissue between the bone and the space for the removed titanium coupon (above). The angular HA crystals are directly incorporated into the bony tissue (Masson, original magnification ×83).

(b)

Figure 6. (continued)

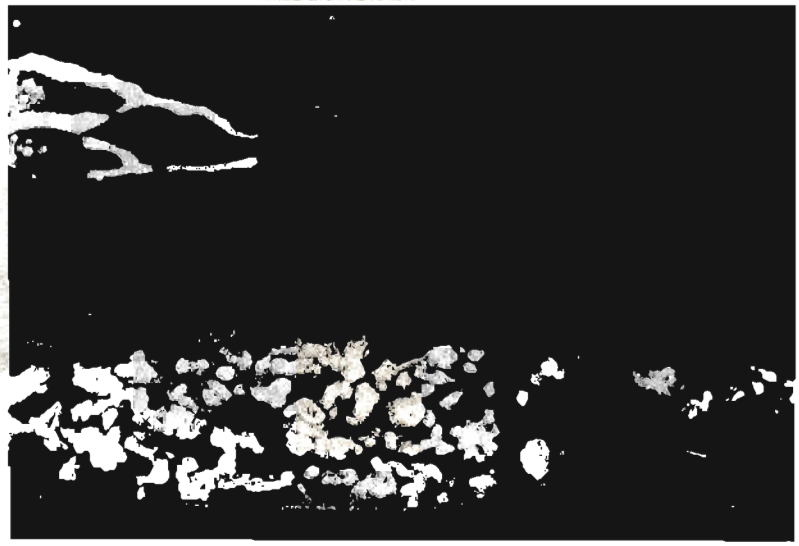

Figure 7. Comparison microradiographs of bone ingrowth into CP-titanium-lined channels at 6 weeks, showing increased bone ingrowth in the channel packed with crystalline-HA grouting (below, with HA powder visible as white particles) versus the unfilled channel (above) (original magnification ×33).

few cell layers thick (Fig. 13). SEM examination of the bone surface adjacent to surface-roughened CP titanium at 12 weeks revealed a thin fibrous tissue covering of the ingrown trabecular bone, with occasional projection of trabeculae through the thin fibrous interface layer (Fig. 14). The titanium plate had some acellular fibrous debris and marrow elements, but no distinct cellular connective tissue covering.

Twenty-five plasma-HA-coated channel specimens and 6 CP titanium channel specimens were mechanically tested in tension to determine the adhesion strength between the channel walls and the ingrown tissue (Table I). The plasma-HA-coated specimens included (a) 10 samples at 6 weeks, 5 of which included crystalline-HA grouting within the channels; and (b) 15 samples at 12 weeks, 8 including grouting. All 6 CP titanium samples were 12-week, and all but one included the crystalline-HA grouting. The reason why only 6 CP titanium channels could be tested was that at least one of the coupon–bone interfaces of most of these samples (including all of the 6-week samples) became disrupted during the minimal amounts of manipulation necessary to remove the intact specimens from the polyethylene chambers. This indicated that the adhesion strengths in these samples was close to zero. The one 12-week CP titanium sample tested failed at 3.66 N, and the CP titanium specimens with crystalline-HA grouting failed at an average of

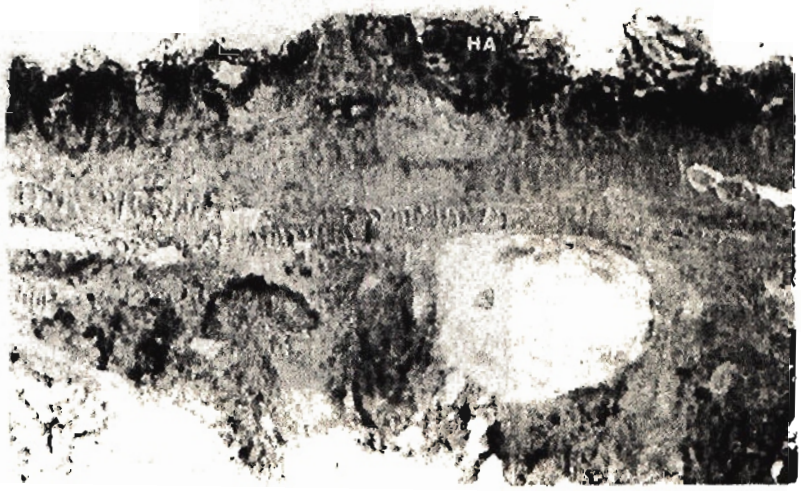

(a)

Figure 9. Illustration of the bone/plasma-HA interface. (a) Photomicrograph showing direct attachment of of the bone to the remaining HA (HA, stained dark, above), with no interposing layer (H & E, original magnification ×529). (b) Microradiograph demonstrating cellular trabecular bone in direct contact with the intact HA layer (original magnification ×212).

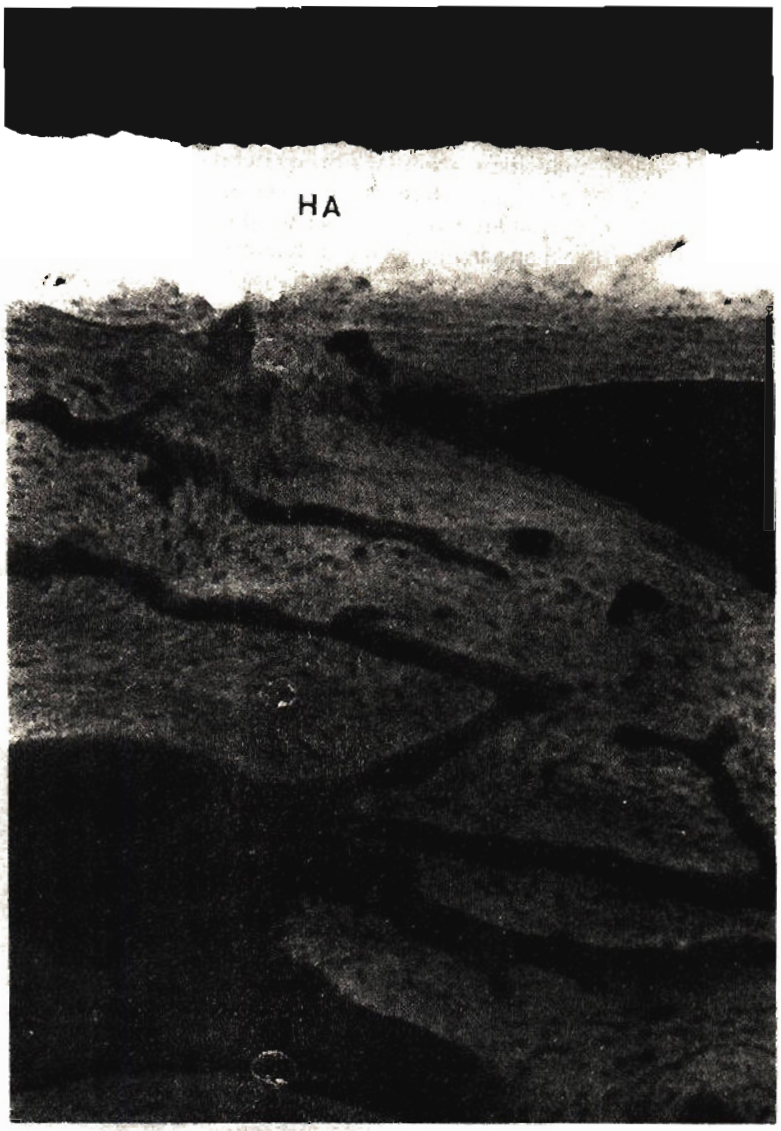

(b)

Figure 9. (continued)

8.88 N. The 6-week unfilled plasma-HA-coated samples failed at 15.29 N, and the 12-week samples failed at 44.81 N. Of the plasma-HA-coated channels with crystalline-HA grouting tested, the 6-week samples failed at 23.00 N, and the 12-week samples failed at an average of 35.56 N.

Figure 10. Photomicrograph showing a HA particle surrounded by bone without any intervening layer. Although the brittle HA is fragmented by the microtome during the slide preparation, the fragments adjacent to surrounding bone remain attached (arrows) (Masson, original magnification ×529).

Analysis using an unpaired Student *t*-test showed no significant difference in failure strengths between the presence or absence of the crystalline-HA grouting in the plasma-HA-coated specimens at both 6 and 12 weeks. A significant increase ($p = .002$) was found in failure strengths of the plasma-HA-coated specimens at 12 weeks vs. the 6-week samples. Visual examination of the specimens following mechanical testing revealed that the failure strengths of the specimen sandwiches paralleled the relative amount of HA pulled off the coated specimen plates. SEM analysis of the specimens postfailure revealed evidence of bone trabeculae directly attaching to the plasma-sprayed HA coating, with specimen failure along the titanium–HA interface and across the HA–tissue interface (Fig. 15). These scanning electron micrographs are further confirmation of the direct attachment of the ingrown bone to the plasma-HA surface, in comparison to the thin interposing soft-tissue layer between the ingrown bone and the bare CP titanium surface previously described.

DISCUSSION

This study presents the initial observations on a new animal model which examines the process of intramedullary bone ingrowth in response to different test materials within a similar bony environment. Differences in the af-

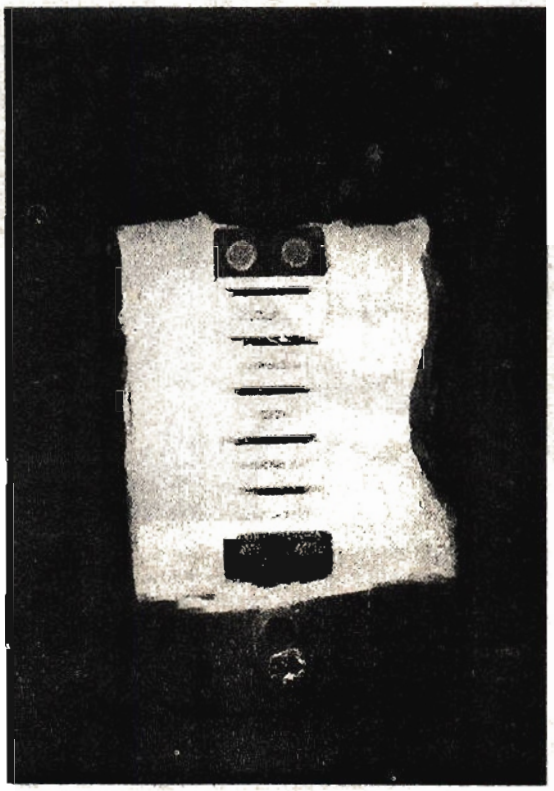

Figure 11. High-resolution Faxitron x-ray of intact 12-week implant with surrounding bone intact, demonstrating complete bone ingrowth across all plasma-HA-lined channels, with only 40-50% filling of the alternating CP-titanium-lined channels

finity of bone for various test materials as measured by the speed, amount, and quality of bone ingrowth can be measured. This model also allows for a detailed analysis of the bone–implant interface. It was designed to resemble the *in vivo* location of orthopedic implants more closely than current models studying bone ingrowth, such as the transcortical plug model, popularized by many authors.[2,6,9,30,34] In the transcortical plug model, cylinders of test materials are placed through drillholes in the diaphysis of long bones. Specimens are analyzed both histologically, to examine the extent of bone ingrowth into porous specimens and to view the bone–implant interface, and mechanically, by pushout testing of the shear strength and stiffness of the bone–implant interface.

The bone response to the transcortical plug model is primarily one of cortical bone, and the results of these studies reflect the ingrowth and at-

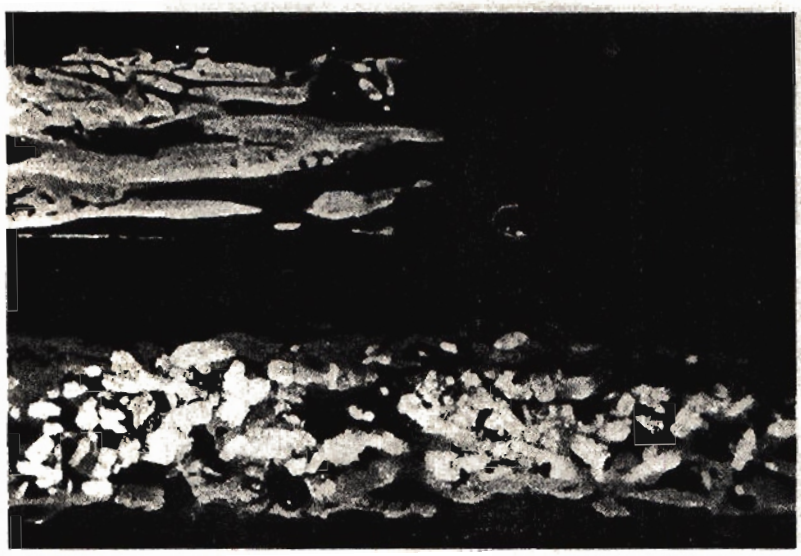

Figure 12. Comparison microradiographs of bone ingrowth into CP-titanium-lined channels at 12 weeks, with (below) and without (above) the presence of crystalline-HA grouting. By 12 weeks, bone can be seen along the edges of the unfilled and filled channels, with increased ingrowth in the presence of the HA (original magnification ×33).

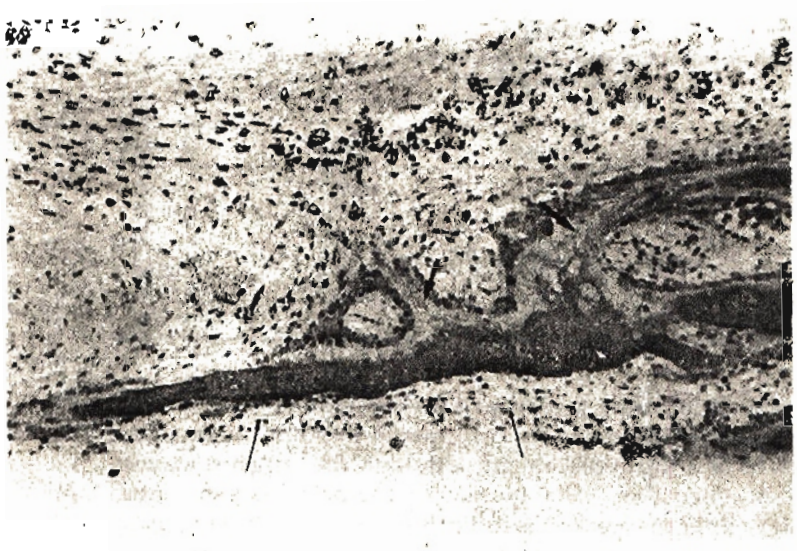

Figure 13. Photomicrograph of the edge of the ingrown bone adjacent to a rough-surface CP titanium plate (removed) at 12 weeks, showing a thin layer of fibrous tissue (thin arrows) between the bone and the free edge. Note the osteoid (lighter staining at thick arrows) and active osteoblasts covering most bone surfaces at 12 weeks, in contrast to the smooth-surfaced 12-week specimens (original magnification ×212).

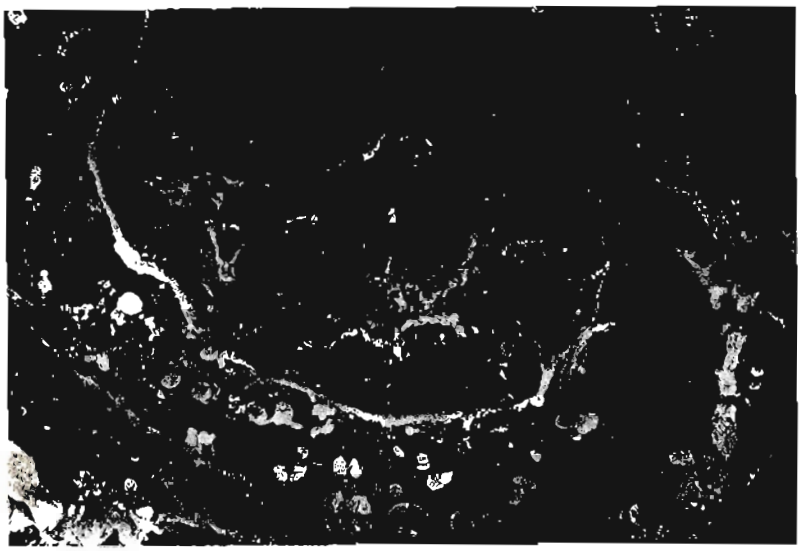

Figure 14. SEM of the bone side of the bone-titanium interface showing a bony trabeculum projecting through the thin fibrous tissue layer. The trabeculum is surrounded by marrow-derived blood cells, and its surface architecture is similar to the surface of the roughened CP titanium test coupons (original magnification ×500).

TABLE I
Force to Failure of Intact Coupon–Tissue–Coupon Specimens in Tension
(Newtons ± S.D.)

Number of Weeks	Titanium	Titanium + Ostergen	Plasma-HA	Plasma-HA + Osteogen
6	—	—	15.29 ±3.03 (n = 5)	23.00 ±16.32 (n = 5)
12	3.68 (n = 1)	8.88 ±6.4 (n = 5)	44.81 ±15.54 (n = 7)	35.56 ±18.99 (n = 8)

tachment of a transcortical injury response in the presence of these test materials. In the clinical situation of an orthopedic implant, such as the femoral component of a hip replacement, although the surgeon may attempt to fill the intramedullary canal by placing the prosthesis in contact with cortical bone, a uniform press-fit is difficult if not impossible to obtain. Clinical reports have pointed out that typically only 10–15% of the stem surface is within 1 mm of the cortical bone and 20–30% within 1 mm of the cancellous bone; therefore, most of the implant resides in a region more than 1 mm distant from cancellous or endosteal bone.[35] In fact, it may be that the desired bone response needed for stable fixation of either a porous-

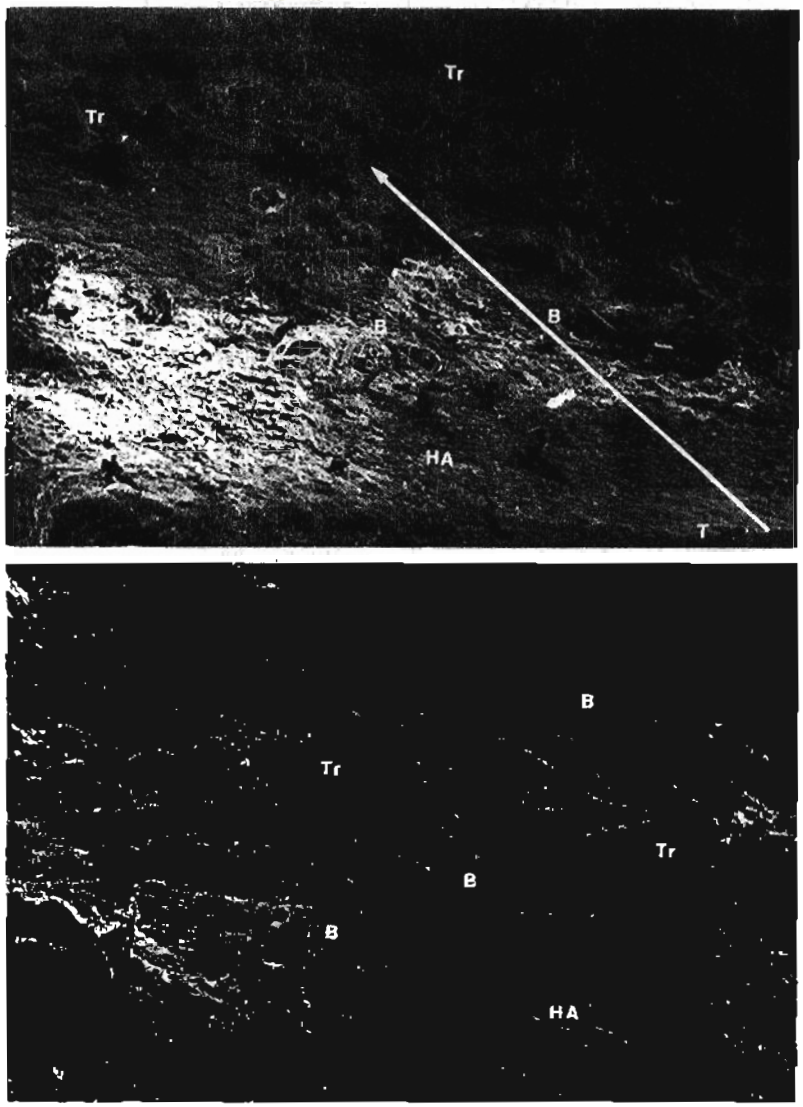

(a)

(b)

Figure 15. Scanning electromicroscopy of the failure surface of a 6-week sample. (a) Low-power SEM across the entire failure surface. The failure pattern follows the long arrow, beginning at the titanium–HA interface, propagating through the HA, then through the HA–bone interface, and finally across the thin bony trabeculum towards the center of the channel. The channel in this micrograph was open to the intramedullary space along the bottom and to the right (original magnification ×35). (b) Higher power SEM through the failure at the HA–bone interface, showing a continuum from HA to bone with no intervening soft-tissue layer. This represents direct bone bonding to the HA, as failure occurs through this interface, not along it (T = CP titanium, HA = plasma-HA coating, B = bone, Tr = failure through trabeculae) (original magnification ×150).

coated device (relying on bone ingrowth) or a biological fixation device (relying on stable and secure direct bone attachment) comes from the intramedullary cancellous bone and endosteum. In our new model, although the chamber is implanted through a cortical window, the ingrowth channels are open only to the intramedullary environment of the metaphysis, with the nearest aspect of the channel opening being 2 mm from the cortical surface. Also, a 1-mm lip was built into the outer aspect of the chamber, to seal off the bony defect and prevent any infolding of periosteum. The fact that a truly intramedullary bone response was observed is indicated by the fact that the bone ingrowth into the channels was found to be symmetric across the channel openings, with equal amounts of bone ingrowth in the most superficial and the deepest edges of the channels.

Although the push-out test with a transcortical plug has become the de facto standard for evaluating implant–bone mechanical interactions, this same model has been criticized for its many disadvantages and sources of experimental error.[36] The transcortical plug push-out test, which loads the interface in shear, is heavily dependent upon the surface roughness of the implant and the unknown level of radial stress present in the specimen prior to testing. It is also extremely sensitive to any tapering in the specimen and possible mechanical blocks caused by periosteal bone overgrowth. Testing to failure in tension, as is done in our model, is not dependent upon surface roughness, provided that the surface is not porous. In situations where failure occurs at the implant–bone interface, the true adhesion of the surfaces can be determined with this method. When failure occurs through either of the two materials (implant or bone), the combined state of stress established in the push-out test complicates the determination of a failure stress, if not making its determination impossible, because of the unknown radial stress. In the tensile test used in our model a state of plane strain is produced, inducing a perpendicular stress that can be computed from linear elasticity theory and factored into the computed failure stress determination. However, with failure through the coupon–bone interface, the materials properties mismatch between the bone and the test coupon creates a stress discontinuity and is an unavoidable source of error in any interface model system.

Implantable chambers have been used in the past for the study of various physiologic processes and responses of bone tissue, including basic bone physiology and circulation,[16] normal bone healing,[17,18,21] and bone response to osteogenic factors[19] and implant materials such as bone cement.[20] In all these studies, long-term implantable chambers made of CP titanium with a single ingrowth channel are used, and the response of cortical or cancellous bone is studied. Although the use of titanium as the chamber material is preferred by these authors because of its known biocompatibility, the actual effect of the metal on the bone responses being studied has never been fully examined. UHMW polyethylene was chosen as the material of the implant chamber in this model for four reasons. First, it is readily available and machinable. Second, it is known to be biocompatible and is currently used as a component of many orthopedic implants. Also, it is radiolucent, and it

allows for x-ray examination of the ingrown bone with the implant maintained intact. Finally, it is nonmetallic, and thus can accommodate metal test coupons without the problem of possible galvanic effects.

The width of the ingrowth channels in the new model is 1 mm. This is the same as the diameter of the ingrowth canal in the bone chamber used by Kalebo and Jacobsson, who studied the healing capacity of the rabbit tibial metaphysis.[18] In studies of vital microscopy of bone, slit gaps of 100–150 μm are utilized, and bone ingrowth across a 4-mm-long channel is observed.[16,17] Gaps of only 70 μm were associated with the ingrowth of fibrous tissue instead of bone tissue.[16] The width and depth of the channels were chosen after reviewing the x-rays of a number of adult mongrel dog femurs, as measurements indicated that this size could be easily inserted and would occupy a majority of the intramedullary space in the lateral view.

The results of the group I animals suggests an initial response to surgical trauma with abundant bone ingrowth at 6 weeks, followed by a decrease in ingrown bone, remodeling of the existing bone to a more mature state, and later resorption. Little difference was found among the four test groups in terms of the amount of bone ingrowth and the ability of any of the test materials to slow or prevent the bone resorption seen at 24 weeks. The only significant finding was the increased initial ingrowth seen in the sputter-HA-coated channels, but this effect was lost by 12 weeks.

The bone resorption seen by 24 weeks may be due in part to the minimal mechanical stresses seen by the implant chamber in the absence of direct bony contact or interlocking with the implant materials. This possibility is also suggested by the results of the group II dogs, where the implant was directly attached to the ingrown bone by the plasma-HA-coated samples, and significantly increased bone ingrowth was noted in the CP titanium samples at 12 vs. 6 weeks. No animals in this group were taken to 24 weeks, so a complete comparison cannot be made. This pattern of late resorption may also be due to the polished surfaces used in the group I animal test coupons, which have been shown previously to favor fibrous tissue encapsulation preventing direct bone–implant contact in the transcortical model.[32] In the group II animals, only surface-roughened test coupons were used, and increased ingrowth was noted at 12 weeks as compared to 6 weeks for all four test groups.

In our new model, only the openings of the ingrowth channels are placed adjacent to the intramedullary endosteal bone, the bulk of the actual test material surfaces being at a distance from bone initially. This is in contrast to the the transcortical plug model, where the entire implant surface is initially in direct contact with bone. The ingrowth channels in our model first fill with blood, which is rapidly organized to a loose connective tissue at the same time that bone begins to grow in from the channel openings. A competition for the implant surface between bone and fibrous tissue ensues, and material properties and surface properties of the channel walls combine to favor one cell type over the other. In the group I dogs, the smooth surface strongly favored the formation of a fibrous tissue interface. In the group II dogs, the surface-roughened test coupons did not favor fibrous tis-

sue, and the CP titanium channels showed areas of direct bone apposition at 12 weeks.

The plasma-HA surface coating in the group II dogs was associated with greatly increased bone ingrowth at both 6 and 12 weeks. Calcium phosphate ceramic coatings are well known to promote bone ingrowth and direct bone bonding.[2,7-9,15] This new model is well suited to studying various different coating techniques, to allow for direct comparisons in terms of intramedullary bone response and the strength of the bony attachment in the early phases of tissue healing and bone–implant interface formation.

The presence of the crystalline HA grouting material within the ingrowth channel, even in the absence of a bone-enhancing coating on the metal, was associated with a large increase in bone ingrowth versus unfilled channels having identical titanium lining coupons. This result points out not only the bone conductive properties of the material tested, but also the potential use of this model in the study of various osteoconductive or osteoinductive materials including growth factors which may prove useful for the newer strategies of implant fixation.

The mechanical testing data indicate a strong adhesion between the ingrown bone and the plasma-HA coating. The SEM observations of failure *along* the titanium–HA interface and *across* the bone–HA interface suggests that the bone–HA interface is the stronger of the two. To convert the force to failure into failure strength, the actual area of bone–HA contact is needed. For the 12-week samples, histologic and radiographic evaluation showed bone ingrowth spanning the length of the channel. A minimal value for failure strength can be estimated based on complete contact of the HA coating and the ingrown bone. For a force to failure of 44 N, a surface area of 40 mm^2 (the maximal available area of the channel wall) calculates to a failure strength of 1.1 MPa. This minimum value is similar to the findings of Søballe and coworkers for push-out failure strengths of plasma-HA coated porous coated implants in cancellous bone of the canine distal femur.[37] Reports of failure strengths of the cortical bone–plasma-HA interface using the transcortical model are significantly higher.[2,7-9] In the 6-week samples, complete bone ingrowth is not seen, so that the lower force to failure in these samples reflects less surface area of the bone–HA interface rather than a lower force per unit area.

A force to failure in the 12-week titanium channels with the crystalline-HA grouting of 9 N implies a failure strength of 0.0225 MPa, assuming complete bone ingrowth into the channel. This reflects the strength of the titanium–bone interface at 12 weeks, since no crystalline-HA was seen along the plane of failure interposed between the titanium and the ingrown bone. The lack of measurable strength in the 6-week titanium channels and the unpacked 12-week titanium channel probably reflects the significantly less bone ingrowth and subsequent bone–titanium interface seen in these channels.

Our new model provides some evidence for the concept of titanium osteointegration, as proposed by Albrektsson and others.[24,25,28] In all of these ultrastructural studies of the bone–titanium interface, the test metal was

implanted in direct initial contact with bone. Titanium is known to be quite biocompatible, and many believe that bone might actually bond directly to its oxide surface.[24] In our model, however, the titanium surface was placed at a distance from the bone, and the ingrowing bone had to displace the fibrous tissue layer which formed initially at the coupon surface. In a clinical study of osteointegration, the failures of direct bone bonding were attributed to inadequate primary contact of the implant with bone, as was the situation in this model.[38] SEM observation of the bone surface adjacent to surface-roughened CP titanium at 12 weeks revealed areas of trabecular projection through the thin fibrous interface layer. Although the exact area of contact on the titanium plate could not be identified, direct contact between the projecting trabeculum and the titanium can be inferred from the lack of an organized cellular layer on the corresponding titanium plate surface.

Bone growth and remodeling are known to respond to physiologic mechanical forces. However, these forces are difficult to measure *in vivo* and impossible to accurately control. For the purpose of examining the bone response to specific implant materials under controlled conditions, it may be desirable to eliminate mechanical force as a variable. In our experimental model, bone is not placed in direct contact with the experimental surface under compressive force, as is the case in many models. Thus, the bone that has grown into the chambers has done so in an absence of mechanical forces. Since most orthopedic implants that rely in bone bonding or ingrowth are allowed an initial period of decreased loading (non-weight-bearing), this model is not unrealistic. Also, proponents of osteointegration note that an initial period of complete stability without load is necessary for successful bone bonding, and encapsulation by connective tissue is likely following immediate loading.[24]

CONCLUSIONS

(1) A new experimental animal model has been developed to study the response of intramedullary bone to various test materials and surfaces, utilizing an implantable UHMW polyethylene chamber containing multiple bone ingrowth channels lined by coupons of various materials and surfaces to be tested. The model also allows for a detailed analysis of the bone–implant interface.

(2) A comparison of smooth-surface coupons of titanium, titanium alloy, sputter-HA-coated titanium alloy, and UHMW polyethylene revealed little difference in the pattern of early abundant bone ingrowth and later remodeling and resorption, except for a significant increase in early bone ingrowth in the sputter-HA-coated samples. In all cases the blood initially filling the channels rapidly converts to a fibrous tissue closely adherent to the smooth-surfaced coupons, and no significant bone attachment to the coupon surfaces is noted.

(3) A comparison of rough-surfaced coupons of titanium with or without a plasma-sprayed HA coating revealed increased bone ingrowth in the HA-

lined channels at 6 weeks and a further increase by 12 weeks, with evidence of direct bone bonding to the HA coating. This bone–HA interface showed a stronger attachment strength than the metal–HA interface, which failed first when mechanically tested in tension. A thin layer of fibrous tissue was present at the coupon surface for most of the titanium samples, which had little adhesion strength, although some areas of bone directly adjacent to the titanium were observed.

(4) A crystalline-HA grouting material promoted increased bone ingrowth at both 6 and 12 weeks, was directly incorporated by the ingrown bone, and promoted some mechanical stability of the bone–titanium interface at 12 weeks.

The authors gratefully acknowledge the help of Hubert Sissons, M.D. in the interpretation of the histologic material, and the assistance of Robert Casar in the design and execution of the mechanical testing. This work was supported by grants from the Orthopaedic Research and Education Foundation, the David L. Klein Research and Education Endowment, and the Anne and Harry Reicher Foundation.

References

1. R. J. Haddad Jr., S. D. Cook, and K. A. Thomas, "Biological fixation of porous-coated implants," *J. Bone Jt. Surg.*, **69A**, 1459–1466 (1987).
2. R. G. T. Geesink, K. De Groot, and C. P. A. T. Klein, "Chemical implant fixation using hydroxyl-apatite coatings," *Clin. Orthop. Rel. Res.*, **225**, 147–170 (1987).
3. J. C. Chae, J. P. Collier, M. B. Mayor, and V. A. Surprenant, "Efficacy of plasma-sprayed tricalcium phosphate in enhancing the fixation of smooth titanium intramedullary rods," *Ann N.Y. Acad. Sci.*, **523**, 81–90 (1988).
4. J. A. Longo, F. P. Magee, S. E. Mather, R. A. Yapp, J. B. Koeneman, and A. M. Weinstein, "Comparison of HA and non-HA coated carbon composite femoral stems," Transactions of the 35th Annual Meeting of the Orthopaedic Research Society, Las Vegas, Nevada, 384, 1989.
5. J. L. Berry, J. M. Geiger, J. M. Moran, J. S. Skraba, and A. S. Greenwald, "Use of tricalcium phosphate or electrical stimulation to enhance the bone-porous implant interface," *J. Biomed. Mater. Res.*, **20**, 65–77 (1986).
6. R. C. Anderson, S. D Cook, A. M. Weinstein, and R. J. Haddad Jr., "An evaluation of skeletal attachment of LTI pyrolytic carbon, porous titanium, and carbon-coated porous titanium implants," *Clin. Orthop. Rel. Res.*, **182**, 242–257 (1984).
7. R. G. T. Geesink, K. De Groot, and C. P. A. T. Klein, "Bonding of bone to apatite-coated implants," *J. Bone Jt. Surg.*, **70B**, 17–22 (1988).
8. S. D. Cook, K. A. Thomas, J. F. Kay, and M. Jarcho, "Hydroxyapatite-coated titanium for orthopedic implant applications," *Clin. Orthop. Rel. Res.*, **232**, 225–243 (1988).
9. S. D. Cook, K. A. Thomas, J. F. Kay, and M. Jarcho, "Hydroxyapatite-coated porous titanium for use as an orthopedic biologic attachment system," *Clin. Orthop. Rel. Res.*, **230**, 303–312 (1988).
10. F. C. M. Driessens, "Formation and stability of calcium phosphates in relation to the phase composition of the mineral in calcified tissues," In *Bioceramics of Calcium Phosphate*, K. De Groot (ed.), CRC Press, Boca Raton, 1983.
11. M. Jarcho, "Calcium phosphate ceramics as hard tissue prosthetics," *Clin. Orthop. Rel. Res.*, **157**, 259–278 (1981).

12. M. Jarcho, J. F. Kay, K. I. Guaer, and R. H. Doremus, "Tissue cellular and subcellular events at a bone-ceramic hydroxyapatite interface," *J. Bioeng.*, 1, 79–92 (1977).
13. M. M. Walker and J. L. Katz, "Evaluation of bonding of bone to inorganic crystal surfaces," *Bull. Hosp. Joint Dis. Orthop. Inst.*, 43(2), 103–108 (1983).
14. P. Ducheyne, L. L. Hench, A. Kagan Jr., M. Martens, A. Bursens, and J. C. Mulier, "Effect of hydroxyapatite impregnation on skeletal bonding of porous coated implants," *J. Biomed. Mater. Res.*, 14, 225–237 (1980).
15. J. R. Parsons, J. L. Ricci, P. Liebrecht, R. L. Salsbury, A. S. Patras, and H. Alexander, "Enhanced stabilization of orthopaedic implants with spherical hydroxyapatite particulate," in *Biological and Biomechanical Performance of Biomaterials*, P. Christel, A. Meunier, and A. Lee (eds.), Elsevier, New York, 1986, pp. 477–492.
16. T. Albrektsson, "Implantable devices for long-term vital microscopy of bone tissue," *Crit. Rev. Biocompat.*, 3, 25–51 (1987).
17. H. Winet and T. Albrektsson, "Wound healing in the bone chamber 1. Neoosteogenesis during transition from the repair to the regenerative phase in the rabbit tibial cortex," *J. Orthop. Res.*, 6, 531–539 (1988).
18. P. Kalebo and M. Jacobsson, "Recurrent bone regeneration in titanium implants: experimental model for determining the healing capacity of bone using quantitative microradiography," *Biomaterials*, 9, 295–301 (1988).
19. J. J. Benedict, A. B. Prewett, M. N. Kern, W. C. Fox, T. B. Aufdemorte, and J. W. Posner, "The evaluation in primates of a bovine derived osteogenic factor using the analytical bone implant model," Transactions of the 15th Annual Meeting of the Society for Biomaterials, Lake Buena Vista, FL, 125, 1989.
20. T. Albrektsson and L. Linder, "A method for in vivo observations of the cement-bone interface," Proceedings of the 1st World Congress on Biomaterials, Austria, 140, 1980.
21. H. Winet, J. Y. Bao, and R. Moffat, "Control-control bone chamber model for quantitative evaluation of cortical bone primary healing," Transactions of the 35 Annual Meeting of the Orthopaedic Research Society, Las Vegas, NV, 563, 1989.
22. J. E. Lemons, M. W. Wiemann, and A. B. Weiss, "Biocompatibility studies on surgical grade titanium, cobalt, and iron based alloys," *J. Biomed. Mater. Res.*, 7, 549–553 (1976).
23. D. F. Williams, "Titanium and titanium alloys," in *Biocompatibility of Clinical Implant Materials, Volume I*, D. F. Williams (ed.), CRC Press, Boca Raton, 1981.
24. T. Albrektsson, P.-I. Brånemark, H.-A. Hansson, and J. Lindström, "Osseointegrated titanium implants,"*Acta. Orthop. Scand.*, 52, 155–170 (1981).
25. L. Linder, T. Albrektsson, P.-I. Branemark, H.-A. Hansson, B. Ivarsson, U. Jonsson, and I. Lundstrom, "Electron microscopic analysis of the bone-titanium interface,"*Acta. Orthop. Scand.*, 54, 45–52 (1983).
26. T. Albrektsson, H.-A. Hansson, and B. Ivarsson, "Interface analysis of titanium and zirconium bone implants," *Biomaterials*, 6, 97–101 (1985).
27. T. Albrektsson and H.-A. Hansson, "An ultrastructural characterization of the interface between bone and sputtered titanium or stainless steel," *Biomaterials*, 7, 201–205 (1986).
28. C. Johansson, J. Lausmaa, M. Ask, H.-A. Hansson, and T. Albrektsson, "Ultrastructural differences of the interface zone between bone and Ti-6Al-4V or commercially pure titanium," *J. Biomed. Eng.*, 11, 3–8 (1989).

29. N. C. Blumenthal and V. Cosma, "Inhibition of apatite formation by titanium and vanadium ions," *J. Biomed. Mater. Res.*, **23**, 13–22 (1989).
30. J. D. Bobyn, R. M. Pilliar, H. U. Cameron, and G. C. Weatherly, "The optimum pore size for the fixation of porous-surfaced metal implants by the ingrowth of bone," *Clin. Orthop. Rel. Res.*, **150**, 263–270 (1980).
31. S. J. Cook, K. A. Walsh, and R. J. Haddad Jr., "Interface mechanics and bone growth into porous co-cr-mo alloy implants," *Clin. Orthop. Rel. Res.*, **193**, 271–280 (1985).
32. K. A. Thomas and S. D. Cook, "An evaluation of variables influencing implant fixation by direct bone apposition," *J. Biomed. Mater. Res.*, **19**, 875–901 (1985).
33. F. P. Magee, J. A. Longo, and A. K. Hedley, "The effect of age on the interface strength between porous coated implants and bone," Transcripts of the 35th Annual Meeting of the Orthopaedic Research Society, Las Vegas, NV, 575, 1989.
34. K. A. Thomas, J. F. Kay, S. D. Cook, and M. Jarcho, "The effect of surface macrotexture and hydroxylapatite coating on the mechanical strengths and histologic profiles of titanium implant materials," *J. Biomed. Mater. Res* , **21**, 1395–1414 (1987).
35. P. C. Noble, J. W. Alexander, J. A. Maltry, D. T. Yew, and H. S. Tullos, "The myth of a press-fit cementless femoral prosthesis," Presented at the 55th Annual Meeting Amer. Acad. Orthp. Surg., Atlanta, Feb. 4–9, 1988.
36. J. Black, "Push-out tests" (editorial), *J. Biomed. Mater. Res.*, **23**, 1243–1245 (1989).
37. K. Søballe, E. S. Hansen, H. B-Rasmussen, G. I. Juhl, C. M. Pedersen, V. Knudsen, I. Hvid, and C. Bünger, "Enhancement of osteopenic and normal bone ingrowth into porous coated implants by hydroxyapatite coating," Transcripts of the 35th Annual Meeting of the Orthopaedic Research Society, Las Vegas, NV, 554, 1989.
38. L. Linder, A. Carlsson, L. Marsal, L. M. Bjurstein, and P.-I. Branemark, "Clinical aspects of osteointegration in joint replacement: a histologic study of titanium implants," *J. Bone Jt. Surg* , **70B**, 550–555 (1988).

Received November 28, 1989
Accepted April 9, 1990

NOTES

IMPLADENT LTD.
ADVANCING THE SCIENCE OF IMPLANTOLOGY™
19845 FOOTHILL AVENUE, HOLLISWOOD, NY 11423
BUSINESS (718) 465-1810 TOLL FREE (800) 526-9343 FAX (718) 464-9620